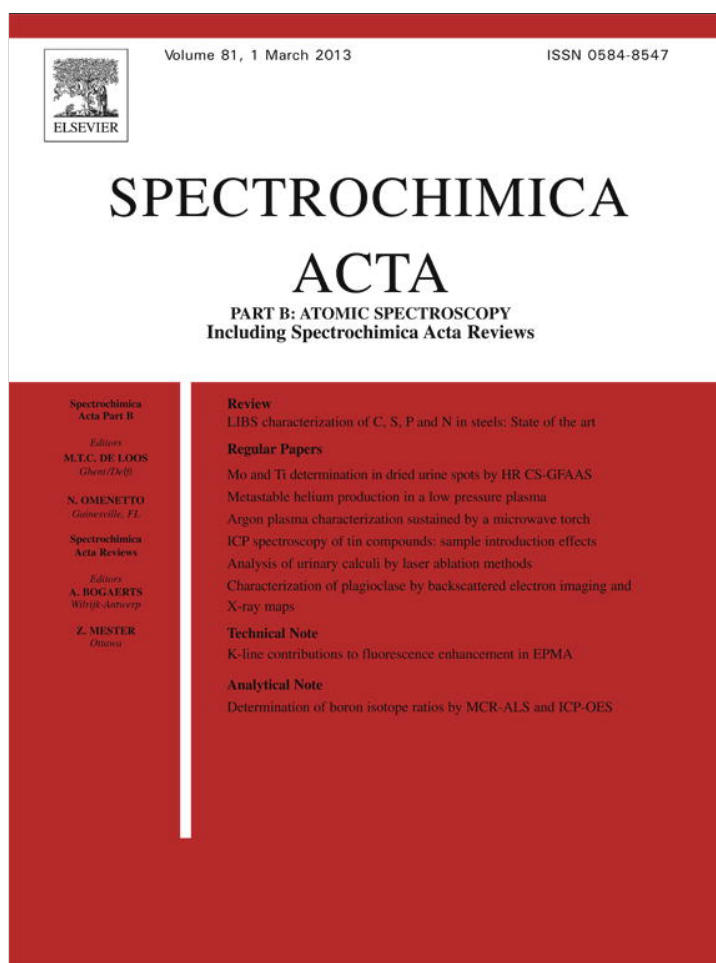


Provided for non-commercial research and education use.  
Not for reproduction, distribution or commercial use.



This article appeared in a journal published by Elsevier. The attached copy is furnished to the author for internal non-commercial research and education use, including for instruction at the authors institution and sharing with colleagues.

Other uses, including reproduction and distribution, or selling or licensing copies, or posting to personal, institutional or third party websites are prohibited.

In most cases authors are permitted to post their version of the article (e.g. in Word or Tex form) to their personal website or institutional repository. Authors requiring further information regarding Elsevier's archiving and manuscript policies are encouraged to visit:

<http://www.elsevier.com/copyright>



Contents lists available at SciVerse ScienceDirect

## Spectrochimica Acta Part B

journal homepage: [www.elsevier.com/locate/sab](http://www.elsevier.com/locate/sab)

Technical Note

## Separate K-line contributions to fluorescence enhancement in electron probe microanalysis

L. Venosta<sup>a</sup>, G. Castellano<sup>a,b,\*</sup><sup>a</sup> FaMAF, Universidad Nacional de Córdoba, Medina Allende s/n, Ciudad Universitaria, (5016) Córdoba, Argentina<sup>b</sup> Consejo Nacional de Investigaciones Científicas y Técnicas (CONICET), Argentina

## ARTICLE INFO

## Article history:

Received 27 July 2012

Accepted 20 December 2012

Available online 5 January 2013

## Keywords:

EPMA

ZAF corrections

Fluorescence enhancement

## ABSTRACT

The behaviour of the fluorescence enhancement correction factor in electron probe microanalysis, as a function of incident electron energy and take-off angle, is assessed for different binary samples in a wide range of compositions. Monte Carlo simulations are employed to validate Reed's correction algorithm [S.J.B. Reed, Characteristic fluorescence corrections in electron-probe microanalysis, Br. J. Appl. Phys. 16 (1965) 913–926], by means of estimating the primary excited radiation volume and the volume corresponding to secondary fluorescence generation. Then, Reed's expression for the fluorescence enhancement has been modified to account for  $K\alpha$  and  $K\beta$  line contributions separately. It is clearly shown that in certain cases the assignment of all fluorescent contribution to the  $K\alpha$  lines may be inadequate, particularly when trace element analysis imposes an accurate determination of elemental concentrations.

© 2012 Elsevier B.V. All rights reserved.

## 1. Introduction

Electron probe microanalysis (EPMA) is a non-destructive technique capable of quantitative chemical analysis at a sub-micron level, using characteristic X-ray intensities emerging from the analysed sample. A powerful technique results when complemented with the acquisition of backscattered electron and secondary electron images, allowing to characterize the sample structure and composition [1]. The technique consists of accelerating electrons toward the sample surface, and recording the emergent X-ray spectrum by means of energy dispersive or wavelength dispersive systems. To achieve quantification it is necessary to have standards of known composition, in order to carry out a correction procedure that relates the intensities measured in an unknown sample with the required concentrations. Since these corrections depend on the concentration values, an iterative procedure must be carried out [2]. To this purpose, different programs have been developed [3].

In matrix corrections, traditionally called ZAF corrections [1], since the fluorescence enhancement correction  $F$  is generally small, usually only the  $K\alpha$  intensities of the enhancing elements are considered [2], because they represent a large fraction of the emitted K radiation. In the present work, the contribution to  $F$  due to the  $K\beta$  line in binary samples is considered according to Reed's approach [4], and certain cases of special interest are shown, in which the omission or the improper assessment of this contribution leads to inaccurate quantification results. These cases are for example when  $K\beta$  is the only K line capable of

producing fluorescence excitement [5], and when the need to determine trace elements [6,7] makes this contribution absolutely necessary to improve the quantification accuracy.

Considerations in the utilization of the correction model generated the need of realizing numeric simulations. Monte Carlo (MC) method [8] has been used in several investigations related to EPMA [9], involving the assessment of electron scattering and X-ray emission for several geometries. MC simulations are very useful to complement experimental results, which allows to validate theoretical models when experimentation is not possible or difficult [7]. In the present work, the PENELOPE routines [10] were used through the PENSLAB main program, provided in the 2003 distribution, with the goal of validating Reed's quantification procedure. This validation was performed by comparing simulated excitation volumes, produced by the incident electrons (primary excitation volume) and the interaction volume of the X-rays corresponding to the enhancing element.

Finally, the contributions to the  $F$  factor due to  $K\alpha$  and  $K\beta$  radiations are calculated and separately studied for some binary samples of interest. Also the behaviour of  $F$  with  $E_0$  and take-off angle is analysed as a function of the concentration of the analysed element  $A$ , for these binary samples.

## 2. Materials and methods

## 2.1. Monte Carlo simulation

In Reed's model it is assumed initially that all primary radiation of the analysed element  $A$  is generated in the surface of the sample, and then an absorption factor is introduced, which accounts for the corresponding ionization depth distribution within the material. This factor is an approximation due to Castaing [11], who assumed an exponential distribution.

\* Corresponding author. FaMAF, Universidad Nacional de Córdoba, Medina Allende s/n, Ciudad Universitaria, (5016) Córdoba, Argentina.

E-mail address: [gcas@famaf.unc.edu.ar](mailto:gcas@famaf.unc.edu.ar) (G. Castellano).

The fluorescence correction is rather insensitive to changes in this function, because its variations are considerably small compared to other factors in the expression for the factor  $F$  [4].

The comparison between the volumes of the excited regions aims to evidence quantitatively the facts pointed out in the previous paragraph. The approach chosen is to define an incident electron range and an enhancement photon range to be compared, the interaction volume in each case being estimated from these definitions. The electron range  $R$  is therefore defined as the depth for which 2% of the incident electrons are transmitted. In the case of the enhancing photons, which will be referred to as “ $B$  photons”, a range  $Q$  is defined such that the ratio between the number of characteristic X-rays reaching the depth  $Q$  and those passing through the range  $R$  is also 2%. To perform this assessment, successive simulations were run for several  $R$  and  $Q$  values, until the desired result was reached.

Simulations were carried out using some of the elements  $B$  of the binary samples for which the  $F$  curves were calculated (Si, Cu, Zn), cases where the correction is significant. An additional simulation was carried out for Zr, which involves the emission of the  $L\alpha$  line. In all cases an enhancement of the  $K\alpha$  line of element  $A$  is considered, the one usually involved in quantification.

The material data files which serve as an input data for this procedure were constructed for pure  $B$  material in order to simplify the routine, since the electron behaviour is very similar in elements whose atomic numbers differ in one or two [2]. Furthermore, fluorescence enhancement becomes important when the sample is rich in element  $B$  [7, 12], which implies that the X-ray interactions are dominated by the presence of element  $B$ . In this manner, when considering an Al–Si sample, the simulation performed corresponds to pure Si, and so on for the rest of the samples. To illustrate an important experimental case, a simulation for Zr was included, using parameters corresponding to a Si–Zr sample.

The parameters of interest in the input file are: simulation time, incident electron energy, the energy below which the electron cannot ionize  $B$  atoms ( $K$  binding energy of  $B$  in the first cases, and  $L_3$  binding energy in the latter), and the threshold energy of  $B$  photons above which  $A$  fluorescence can be excited ( $K$  binding energy of  $A$  in every case). The last two parameters ensure minimization of the CPU calculation time.

Simulation time is determined when the required error is set, less than 10%, which results sufficient for the sought rough estimates. Therefore, the calculations for  $R$  turned out to be from one to six hours, whereas the simulations corresponding to range  $Q$  took from ten to one hundred hours using a Quadcore 2.3 GHz processor, and 4 Gb of RAM.

## 2.2. Fluorescence enhancement

Employing the most frequently used Reed's model, a program written in Pascal was utilized to calculate the contribution to fluorescence correction by the  $K\beta$  line of element  $B$  in binary samples [13]. To this purpose, the expression given by Reed [4] was used with the parameters modified to adequately account for  $K\beta$  radiation.

The program used along this work was developed with the aim of comparing the different ZAF correction models which use several mathematical expressions for the function  $\phi(\rho z)$  [8]. It is a modular program, containing a main menu that allows to choose between multiple options, the most important being the correction models for atomic number, absorption and fluorescence. Once the model has been chosen, an input data file is required, with information about the binary samples and experimental details about how the measurements were carried out: atomic numbers,  $A$ -element concentration, line used for quantification, electron beam energy and take-off angle.

In the present paper, the models which have shown to be more successful [14] were chosen: to correct for the combined effect of absorption and atomic number  $Z_A$ , the Gaussian model [15] modified by Riveros and coworkers [13] was set, Reed's model being chosen for the fluorescence factor  $F$  [4]. The mean ionization potential expression by Brizuela and

Riveros [16], and Bishop backscattering coefficient [17] were also taken into account. Finally, mass absorption coefficients were calculated by means of Heinrich's algorithm [18].

The correction due to  $K\alpha$  line intensity was compared with the one due to  $K\beta$ , running the program for each separate case, using the binary samples shown in Table 1 (the take-off angle is  $35^\circ$  in all cases). Typical  $E_0$  values in EPMA have been chosen for each sample, trying to use always an energy twice greater than the  $A$ -element shell's binding energy.

The behaviour of the fluorescence factor  $F$ , as a function of the concentration of the enhanced element  $A$ , was also studied for several values of  $E_0$  and take-off angles. To this aim, the intensities of both  $K$  enhancing lines were used. The same samples that were used to compare the corrections were taken into account. In addition, Ni–Cu samples were studied, since it is a very important case because Cu- $K\beta$  line only is responsible for enhancement of Ni.

## 3. Results and discussion

The MC simulation values obtained for the  $R$  and  $Q$  ranges, corresponding respectively to electron and X-ray transmission, are shown for each element in Table 2. The uncertainties included in these results are three times the standard deviation, as reported by the program PENSLAB. Differences between the uncertainties associated to the electron and X-ray transmitted fractions respectively corresponding to  $R$  ( $TE$ ) and  $Q$  ( $TP$ ) are due to the fact that X-ray generation by the incident electrons is an event which has a small probability to occur: typically only one of 1000 electrons produces a vacancy in the  $K$  shell [2], and the vacancies yielding characteristic X-rays are given by the factor  $\omega$ . To achieve a statistically valid result, a long simulation time is thus required. The number of incident electrons is determined by the length of the simulation, and in a relatively short period of time a large number of electrons transmitted across the range  $R$  is obtained, which reduces the statistical uncertainty to 1% in every case. In general, the uncertainty in  $TP$  ( $Q$  range) is less than 10%. As can be seen, in the case of Cu- $K\beta$  and Zr- $L\alpha$ , the smaller intensities of the lines used to define  $Q$  demanded a larger simulation time.

The uncertainties in the number of transmitted particles are inherent to the stochastic nature of the paths simulated, and are readily reported by the program PENSLAB [10]. By running similar simulations around the solutions found for the ranges  $R$  and  $Q$ , it was possible to establish linear relationships between these variables and the respective transmitted fractions  $TE$  and  $TP$ , which allowed to assess the corresponding uncertainties by error propagation.

Table 2 evidences important differences between the ranges  $R$  and  $Q$ , which implies a remarkable contrast in the excitation volumes for primary and secondary ionizations, since the volume ratio can be roughly estimated as  $(R/Q)^3$ . The larger the line energy used for fluorescence calculation, the smaller the corresponding volume ratio obtained, because of their higher penetration power, while the exciting electron volume maintains its reduced size. The simulation results clearly allow to corroborate the hypothesis that states that primary radiation is produced at the surface and then attenuated exponentially.

**Table 1**

Binary samples used in the  $F$  factor calculation. Atomic numbers  $Z_A$  and  $Z_B$ ,  $A$ -element binding energy  $E_{C_A}$ , incident beam energy  $E_0$  and  $K\alpha$  and  $K\beta$  line energies for element  $B$  are shown.  $A$  refers to the analysed element, and  $B$  is the enhancing element [19,20].

Samples	$Z_A$	$Z_B$	$E_{C_A}$ (keV)	$E_0$ (keV)	$K\alpha$ (keV)	$K\beta$ (keV)
Al–Si	13	14	1.560	15	1.740	1.836
Cr–Fe	24	26	5.989	15	6.404	7.058
Mn–Co	25	27	6.539	15	6.930	7.649
Fe–Ni	26	28	7.112	20	7.478	8.265
Co–Cu	27	29	7.709	20	8.048	8.905
Ni–Zn	28	30	8.333	20	8.639	9.572

**Table 2**

Simulations results.  $TE$  and  $TP$  are the electrons and X-ray transmitted fractions for  $R$  and  $Q$ , respectively. From the relation between  $TE$  ( $TF$ ) and  $R$  ( $Q$ ) obtained from the simulations, the corresponding uncertainties for the ranges  $R$  and  $Q$  were obtained by error propagation. Between parentheses in the first column, the lines used to perform the calculations in each case are shown. The last two columns indicate the simulation time in hours.

Element	$E_0$ (keV)	$R$ ( $\mu\text{m}$ )	$TE$	$Q$ ( $\mu\text{m}$ )	$TF$	$t_R$ (h)	$t_Q$ (h)
Si (K $\alpha$ )	15	$2.410 \pm 0.003$	$0.0198 \pm 0.0002$	$35.0 \pm 0.2$	$0.019 \pm 0.001$	1	10
Cu (K $\beta$ )	25	$1.630 \pm 0.001$	$0.0197 \pm 0.0001$	$90.0 \pm 0.2$	$0.019 \pm 0.002$	6	96
Zn (K $\alpha$ )	25	$1.800 \pm 0.005$	$0.0193 \pm 0.0002$	$85.0 \pm 0.2$	$0.019 \pm 0.002$	1	15
Zr (L $\alpha$ )	15	$0.900 \pm 0.002$	$0.0190 \pm 0.0001$	$6.50 \pm 0.06$	$0.021 \pm 0.001$	2	24

In order to separately evaluate the K $\beta$  contribution to the  $F$  correction, different assessments were carried out, as described in the previous section. Curves showing the  $F$  factor dependence on element  $A$  concentration are shown in Fig. 1, corresponding to Ni–Zn samples. The lower curve corresponds to the assessment when only the K $\alpha$  line is taken into account, whereas the upper curve represents the complete contribution involving both K $\alpha$  and K $\beta$  lines. The results are displayed according to the uncertainty estimation provided in different previous works [21]. The K $\beta$  line contribution to  $F$  is 4% for values of concentration smaller than 8%; if  $C_A = 0.1$ , which has been taken as a reference value,  $F[\alpha] = 1.299$  and  $F[\alpha + \beta] = 1.343$ , the difference being less than 1% for concentrations greater than 45%.

For the Co–Cu samples, a difference of 4% is reached when the concentration takes the value 5%; for  $C_A = 0.1$ ,  $F[\alpha] = 1.288$  and  $F[\alpha + \beta] = 1.330$ . Similarly, the Fe–Ni samples present a difference of 4% for a concentration of 5%; if  $C_A = 0.1$  the values obtained are  $F[\alpha] = 1.277$  and  $F[\alpha + \beta] = 1.318$ . In the case of Mn–Co samples, the difference is 3% for concentrations below 10%; if  $C_A = 0.1$  the values obtained are  $F[\alpha] = 1.223$  and  $F[\alpha + \beta] = 1.254$ . For the case of Cr–Fe, a similar plot is obtained, the K $\beta$  line contribution to the  $F$  correction is 3% below a concentration value of 10%. In the case of  $C_A = 0.1$ ,  $F[\alpha] = 1.208$  and  $F[\alpha + \beta] = 1.238$  are obtained. Beyond 50% of concentration, the difference between these magnitudes is less than 1%.

These results agree with the fact that the  $F$  correction is larger when the enhancing line is right above the edge of the analysed element, and when the sample is rich in element  $B$ . An important difference is observed in the case of Al–Si, in which the curves are practically indistinguishable: the difference is below 1% even for small concentrations of element  $A$ ; when  $C_A = 0.1$  the values are  $F[\alpha] = 1.064$  and  $F[\alpha + \beta] = 1.066$ . According to Reed, the most important factor in the expression for  $F$  is  $J(A)$  [4]. In the corresponding expression, the factor  $(r_A - 1)/r_A$  remains approximately constant in the atomic range for which  $F$  is considerable, and the same occurs for the atomic weight ratio  $A_A/A_B$ . The fluorescence yield [22] however, changes substantially with atomic

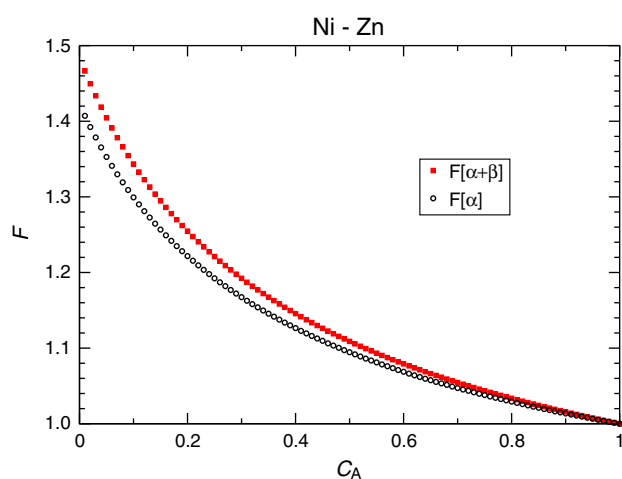


**Fig. 1.** Separate K $\alpha$  line and total K( $\alpha + \beta$ ) line contributions to the fluorescence correction  $F$ , as a function of the concentration of element  $A$  ( $C_A$ ), for Ni–Zn binary samples.

number. K shell values of  $\omega$  for the element  $B$  considered along this work are shown in Table 3.

The small  $\omega$  value for Si relative to the other elements, results in a smaller value for  $F$ . This also is observed in the relative difference between  $F[\alpha]$  and  $F[\alpha + \beta]$ , since these differences are proportional to  $\omega$ . The gap between these curves increases with the concentration of element  $B$  within the sample. This difference is greater than the Al–Si case in the rest of the samples, and its behaviour is similar.

Evaluating  $F$  by taking into account an element  $B$  whose atomic number is that of  $A$ 's increased by one unit, it is seen that despite the value of  $\omega$  is increased, a reduction of the  $F$  factor is obtained up to 8% (comparing Ni–Zn to Ni–Ga) for  $C_A = 10\%$ . This points out the relevance of the mass absorption coefficients in the behaviour of fluorescence correction curves, and allows to interpret why  $F$  varies markedly when  $Z_A$  increases.

It is important to emphasize that the differences evidenced in the previous plots indicate that an important overestimation of the  $F$  factor can be made under the assumption that all enhancing K radiation is K $\alpha$ . For example, if a sample of Cr 10%–Fe 90% is considered, the true value for  $F[\alpha + \beta] = F[\alpha] + F[\beta]$  must be compared to the fluorescence correction factor  $F'[\alpha]$  involving only the  $\alpha$ -line enhancement of element  $B$  and considering the transition rate for  $\alpha$  emission as 100% instead of the corresponding rate (87.6% [23]). This means that instead of the fluorescence correction  $F[\alpha + \beta] = 1.238$  quoted above, one would compute  $F'[\alpha] = 1.208/0.876 = 1.379$ , which implies an overestimation of more than 11% in the value of  $C_A$ . Obviously, this overestimation worsens for lower  $A$  concentrations, where the  $F$  correction becomes more important.

In order to study the whole  $F$  factor behaviour as a function of the concentration of element  $A$ , both K lines were involved; the resulting curves for its behaviour are shown in Figs. 2 to 4, as a function of the concentration of the analysed element  $A$ . Several values for the incident electron energy were used, also shown in the figures. In general, greater values of  $F$  are obtained when  $E_0$  increases, for low element- $A$  concentrations, while the difference between the curves decreases for high element- $A$  concentrations. In the case of the Fe–Ni samples, there is a difference of 8% between the curves corresponding to 15 keV and 30 keV, for the value  $C_A = 0.1$ . The combined effect of the different factors in Reed's expression [4] can be straightforwardly assessed, obtaining the mentioned difference, as seen in Fig. 2. The observed behaviour is similar for the other combinations of elements analysed. An extreme case is the Al–Si samples: since  $F$  is small, the variation with  $E_0$  is more subtle; for example for  $C_A = 0.1$  the relative variation for the corresponding values of  $F$ , between maximum and minimum energy is as low as 2.5%.

Fig. 3 shows the behaviour of  $F$  for different take-off angles. In this case it is also seen that the difference is remarkable for low

**Table 3**

Fluorescence yields for the different  $B$  elements considered [22].

Element	$Z$	$\omega$
Si	14	0.050
Fe	26	0.340
Co	27	0.373
Ni	28	0.406
Cu	29	0.440
Zn	30	0.474

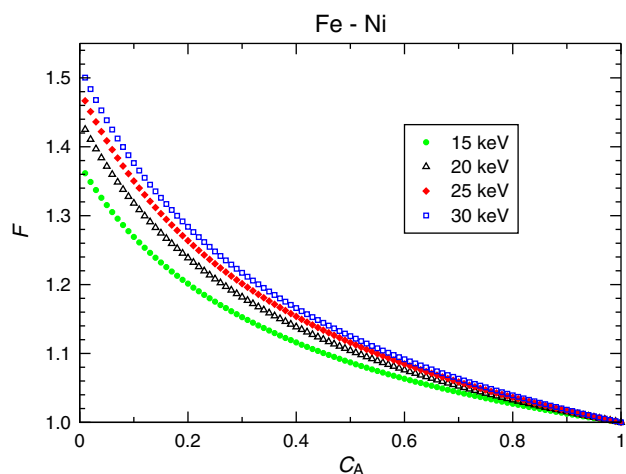


Fig. 2. Fluorescence factor  $F$  as a function of the concentration of element  $A$  ( $C_A$ ), employing several incident-electron energies, for Fe-Ni binary samples. The take-off angle is  $35^\circ$ .

concentrations, and decreases toward large values of  $A$  concentration. This is a consequence of  $F$  being an increasing function of  $C_B$ . Fluorescent intensity travels a shorter path in its way out of the sample, experiencing less attenuation for greater take-off angles, resulting in a larger  $F$  value. As seen in the MC simulations, the characteristic X-ray excitation occurs at greater depths, so when the take-off angle varies, the difference in the path travelled by secondary radiation varies remarkably as compared to the one corresponding to primary radiation.

In Ni-Cu samples, only the  $K\beta$  line obeys the enhancement condition and the results shown in Fig. 4 indicate that the measured intensity is modified by an amount between 5% and 7% for 10% of element  $A$  concentration. Correction due to this line is very important to take into account in measurements involving trace elements [7,12].

#### 4. Conclusions

In this work, the calculation of fluorescence correction taking into account the  $K\beta$  and  $K\alpha$  lines separately has been added to the correction procedure, carefully modifying Reed's correction formulas. The  $K\beta$  contribution to fluorescence correction is shown to be considerable in some cases, and the assignment of all fluorescent contribution to the  $K\alpha$  lines is inadequate for accurate determination of trace element concentrations.

MC simulations were used to validate the hypothesis that secondary excited X-ray volume is considerably greater than the corresponding to

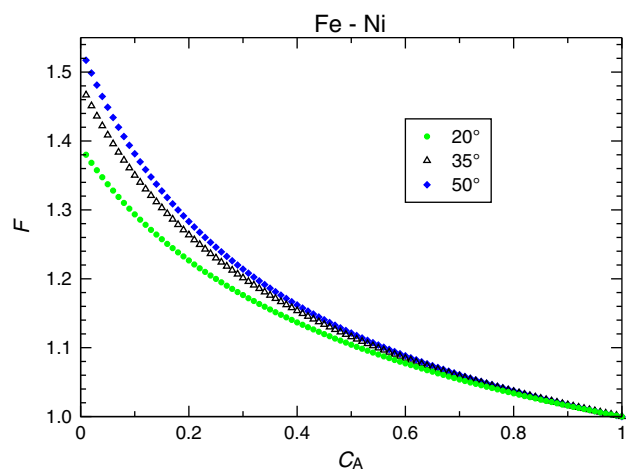


Fig. 3. Fluorescence factor  $F$  as a function of the concentration of element  $A$  ( $C_A$ ), employing three different take-off angles, for Fe-Ni binary samples.  $E_0=25$  keV.

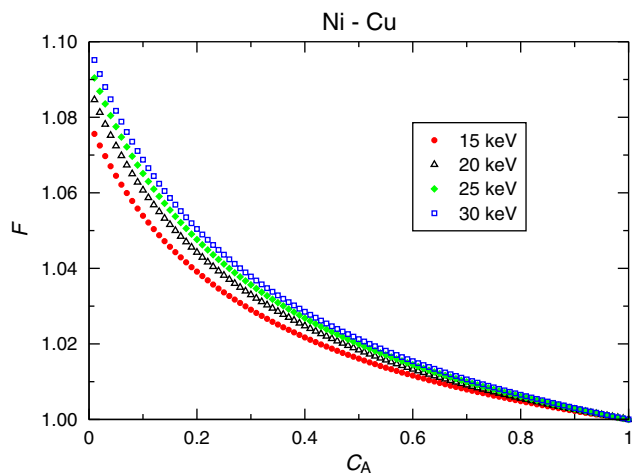


Fig. 4. Fluorescence factor  $F$  as a function of the concentration of element  $A$  ( $C_A$ ), employing several electron incident energies, for Ni-Cu binary samples. Here only the Cu- $K\beta$  line is capable of enhancement. The take-off angle is  $35^\circ$ .

primary X-rays. Additionally, the  $F$  factor behaviour was analysed as a function of concentration, electron beam energy, and X-ray take-off angle. Some cases involving only enhancement by the  $K\beta$  line have also been shown. A remarkable result found along this work is that important overestimations of the  $F$  factor can be made under the assumption that all enhancing K radiation is  $K\alpha$ , with 100% probability for this decay and 0% probability in  $K\beta$  emission. In the cases illustrated here, this inaccuracy may add up to 11% for  $C_A=0.1$ , which would worsen for lower  $A$ -element concentrations.

In early works regarding ZAF corrections, it was essential to minimize calculations, since the assessment of correction factors was extremely time consuming and difficult to achieve. Today an ordinary microprocessor is capable of calculating ZAF corrections practically in an instantaneous way, and the implementation of programmed algorithms makes the correction procedure a straightforward task. The differences brought to evidence here, encourage the implementation of complete  $F$  corrections in order to avoid unnecessary inaccuracies.

#### References

- [1] J. Goldstein, D. Newbury, D. Joy, C. Lyman, P. Echling, E. Lifshin, L. Sawyer, J. Michael, Scanning Electron Microscopy and X-ray Microanalysis, 3rd ed. Springer, New York, 2007.
- [2] S.J.B. Reed, Electron Probe Microanalysis, second ed. Cambridge University Press, Cambridge, 1993.
- [3] J. Trincavelli, G. Castellano, MULTI: an interactive program for quantitation in EPMA, X-Ray Spectrom. 28 (1999) 194–197.
- [4] S.J.B. Reed, Characteristic fluorescence corrections in electron-probe microanalysis, Br. J. Appl. Phys. 16 (1965) 913–926.
- [5] G.L. Fisher, An investigation of electron probe microanalysis corrections in nickel-cobalt alloys, J. Phys. D: Appl. Phys. 4 (1971) 1439–1447.
- [6] Y. Hu, Y. Pan, Method for the calculation of the chemical composition of a thin film by Monte Carlo simulation and electron probe microanalysis, X-Ray Spectrom. 30 (2001) 110–115.
- [7] J.H. Fournelle, S. Kim, J.H. Perepezko, Monte Carlo simulation of Nb  $K\alpha$  secondary fluorescence in EPMA: comparison of PENELOPE simulations with experimental results, Surf. Interface Anal. 37 (2005) 1012–1016.
- [8] V. Scott, G. Love, S. Reed, Quantitative Electron-Probe Microanalysis, second ed. Ellis Horwood Ltd., New York, 1995.
- [9] P. Carpenter, Calculated X-ray intensities using Monte Carlo algorithms: a comparison to experimental EPMA data, Microsc. Microanal. 11 (2005) 1278–1279.
- [10] F. Salvat, J.M. Fernández-Varea, J. Sempau, F. Salvat, J.M. Fernández-Varea, J. Sempau, PENELOPE, A Code System for Monte Carlo Simulation of Electron and Photon Transport, OECD/NEA Data Bank, Issy-les-Moulineaux, France, 2003.
- [11] R. Castaing, Application of electron probes to local chemical and crystallographic analysis, Special Technical Report, California Institute of Technology, Pasadena, CA, July (1955) translated by P. Duwez and D. B. Wittry, from original Thesis published June 8, 1951, University of Paris.
- [12] M. Jercinovic, M. Williams, E. Lane, In-situ trace element analysis of monazite and other fine-grained accessory minerals by EPMA, Chem. Geol. 254 (2008) 197–215.

- [13] J. Riveros, G. Castellano, J. Trincavelli, Comparison of  $\Phi(\rho z)$  curves in EPMA, *Mikrochim. Acta* 12 (Suppl.) (1992) 99–105.
- [14] J. Riveros, G. Castellano, Review of  $\Phi(\rho z)$  curves in EPMA, *X-Ray Spectrom.* 22 (1993) 3–10.
- [15] R. Packwood, J. Brown, Quantitative electron probe microanalysis using Gaussian  $\Phi(\rho z)$  Curves, *X-Ray Spectrom.* 11 (1982) 187–193.
- [16] H. Brizuela, J. Riveros, Study of mean excitation energy and K-shell effect for electron probe microanalysis, *X-Ray Spectrom.* 19 (1990) 173–176.
- [17] H. Bishop, Electron scattering in thick targets, *Br. J. Appl. Phys.* 18 (1967) 703–715.
- [18] K. Heinrich, Mass absorption coefficients for electron probe microanalysis, in: J. Brown, R. Packwood (Eds.), *X-Ray Optics and Microanalysis*, University of Western Ontario, Ontario, 1987, pp. 67–119.
- [19] J.A. Bearden, X-ray wavelengths, *Rev. Mod. Phys.* 39 (1967) 78–124.
- [20] J.A. Bearden, A.F. Burr, Reevaluation of X-ray atomic energy levels, *Rev. Mod. Phys.* 39 (1967) 125–142.
- [21] J. Pouchou, F. Pichoir, Quantitative analysis of homogeneous or stratified microvolumes applying the model “PAP”, in: K. Heinrich, D. Newbury (Eds.), *Electron Probe Quantitation*, Plenum Press, New York, 1991, pp. 31–75.
- [22] M.O. Krause, Atomic radiative and radiationless yields for K and L shells, *J. Phys. Chem. Ref. Data* 8 (1979) 307–327.
- [23] M.-M. Bé, M.-C. Lépy, J. Plagnard, B. Duchemin, Measurement of relative X-ray intensity ratios for elements in the  $22 \leq Z \leq 29$  region, *Appl. Radiat. Isot.* 49 (1998) 1367–1372.